

1 **Deforestation in Amazonia impacts riverine carbon dynamics**

2

3 F. Langerwisch^{1,2}, A. Walz³, A. Rammig^{1,4}, B. Tietjen^{5,2}, K. Thonicke^{1,2}, W. Cramer⁶

4 ¹ Earth System Analysis, Potsdam Institute for Climate Impact Research (PIK), P.O. Box 60 12
5 03, Telegraphenberg A62, D-14412 Potsdam, Germany

6 ² Berlin-Brandenburg Institute of Advanced Biodiversity Research (BBIB), 14195 Berlin,
7 Germany

8 ³ Institute of Earth and Environmental Science, University of Potsdam, Karl-Liebknecht-Str.
9 24-25, D-14476 Potsdam-Golm, Germany

10 ⁴TUM School of Life Sciences Weihenstephan, Land Surface-Atmosphere Interactions,
11 Technische Universität München, Hans-Carl-von-Carlowitz-Platz 2, 85354 Freising,
12 Germany

13 ⁵ Biodiversity and Ecological Modelling, Institute of Biology, Freie Universität Berlin,
14 Altensteinstr. 6, D-14195 Berlin, Germany

15 ⁶ Institut Méditerranéen de Biodiversité et d'Ecologie marine et continentale (IMBE), Aix
16 Marseille Université, CNRS, IRD, Avignon Université, Technopôle Arbois-Méditerranée,
17 Bât. Villemin - BP 80, F-13545 Aix-en-Provence cedex 04, France

18

19 *Correspondence to:* F. Langerwisch (langerwisch@pik-potsdam.de)

20

22 **Abstract**

23 Fluxes of organic and inorganic carbon within the Amazon basin are considerably controlled
24 by annual flooding, which triggers the export of terrigenous organic material to the river and
25 ultimately to the Atlantic Ocean. The amount of carbon imported to the river and the further
26 conversion, transport and export of it, depend on terrestrial productivity and discharge, as well
27 as temperature and atmospheric CO₂. Both terrestrial productivity and discharge are
28 influenced by climate and land use change. To assess the impact of these changes on the
29 riverine carbon dynamics, the coupled model system of LPJmL and RivCM (Langerwisch et
30 al., 2015) has been used. Vegetation dynamics (in LPJmL) as well as export and conversion
31 of terrigenous carbon to and within the river (RivCM) are included. The model system has
32 been applied for the years 1901 to 2099 under two deforestation scenarios and with climate
33 forcing of three SRES emission scenarios, each for five climate models. The results suggest
34 that, following deforestation, riverine particulate and dissolved organic carbon will strongly
35 decrease by up to 90% until the end of the current century. In parallel, discharge increases,
36 leading to roughly unchanged net carbon transport during the first decades of the century, as
37 long as a sufficient area is still forested. During the following decades the amount of
38 transported carbon will decrease drastically. In contrast to the riverine organic carbon, the
39 amount of riverine inorganic carbon is only determined by climate change forcing, namely
40 increased temperature and atmospheric CO₂ concentration. Mainly due to the higher
41 atmospheric CO₂ it leads to an increase in riverine inorganic carbon by up to 20% (SRES A2).
42 The changes in riverine carbon fluxes have direct effects on the export of carbon, either to the
43 atmosphere via outgassing, or to the Atlantic Ocean via discharge. Basin-wide the outgassed
44 carbon will increase slightly, but can be regionally reduced by up to 60% due to deforestation.
45 The discharge of organic carbon to the ocean will be reduced by about 40% under the most
46 severe deforestation and climate change scenario. The changes would have local and regional
47 consequences on the carbon balance and habitat characteristics in the Amazon basin itself but
48 also in the adjacent Atlantic Ocean.

49

50 **1 Introduction**

51 The Amazon basin, defined as the drainage area of the Amazon River, covers approximately
52 six million square kilometres, and more than 70% of it is still covered with intact rainforest
53 (Nobre, 2014). The amount of carbon in biomass in Amazonian rainforest is estimated to be
54 $93 \pm 23 \times 10^{15}$ g C (Malhi et al., 2006). This biomass is stored in a wide range of diverse
55 habitats, including tropical rainforest and savannahs, as well as numerous aquatic habitats,
56 like lakes and wetlands (Goulding et al., 2003; Eva et al., 2004; Keller et al., 2009; Junk,
57 1997). The large diversity in habitats, partly already founded in the geologic formation of
58 Amazonia, leads to a high diversity of animal and plant species (Hoorn et al., 2010), making
59 the Amazon rainforest one of Earth's greatest collections of biodiversity. The Amazon River,

60 which floods annually large parts of the forest, plays an important role in supporting the
61 diversity of Amazonian ecosystems. The flooding is most decisive for the coupling of
62 terrestrial and aquatic processes by transporting organic material from the terrestrial
63 ecosystems to the river (Hedges et al., 2000). The input of terrigenous organic material
64 (Melack and Forsberg, 2001; Waterloo et al., 2006), acts, for instance, as fertilizer and food
65 source (Anderson et al., 2011; Horn et al., 2011), and is a modifier of habitats and interacting
66 local carbon cycles (Hedges et al., 2000; Irmiler, 1982; Johnson et al., 2006; McClain and
67 Elsenbeer, 2001). On a larger scale, the release of carbon from the river into the atmosphere,
68 and its export to the ocean are most relevant factors when it comes to assessing the effects of
69 Amazon ecosystem on climate change. It is estimated that the large scale outgassing of carbon
70 from the Amazon River plays an important role in assessing the future role of the Amazon
71 basin as a carbon sink or source to the atmosphere. Approximately 470×10^{12} g C yr⁻¹ is
72 exported to the atmosphere as CO₂ (Richey et al., 2002), in comparison with about
73 32.7×10^{12} g C yr⁻¹ of total organic carbon (TOC) is exported to the Atlantic Ocean (Moreira-
74 Turcq et al., 2003).

75 Deforestation continues to be the largest threat to Amazonia. The transformation of tropical
76 rainforest to cropland and pasture impacts ecosystem stability profoundly due to altered
77 climate regulation and species richness (Foley et al., 2007; Lawrence and Vandecar, 2014;
78 Malhi et al., 2008; Spracklen et al., 2012). Until the year 2012 approximately 20% of the
79 original forest of the Brazilian part of the Amazon basin has been deforested, corresponding
80 to an area of about 750,000 km² (Godar et al., 2014; INPE, 2013). This deforestation was
81 mainly driven by the land expansion for soybean and cattle production and the expansion of
82 the road network (Malhi et al., 2008; Soares-Filho et al., 2006). Together with climate change
83 effects and forest burning, land cover change is predicted to release carbon at rates of 0.5-
84 1.0×10^{15} g C yr⁻¹ from this area (Potter et al., 2009). Furthermore, the annual CO₂ efflux from
85 pasture soils exceeds that of mature and secondary forest (Salimon et al., 2004). The effects of
86 deforestation on terrestrial carbon storage and fluxes persist several decades after logging
87 because the forest needs about 25 years to recover approximately 70% of their original
88 biomass, and at least another 50 years for the remaining 30% after abandonment of agriculture
89 (Brown and Lugo, 1990; Houghton et al., 2000).

90 Due to the extraction of wood, deforestation leads to immediate changes in the terrestrial
91 organic carbon pools that fuel riverine respiration (Mayorga et al., 2005), increase in velocity
92 and amount of runoff, and discharge (Foley et al., 2002; Costa et al., 2003). Additionally,
93 changes in precipitation caused by climate change alter inundation patterns (Langerwisch et
94 al., 2013) like temporal shifts in high and low water months and changes of inundated area.
95 The combined effects of climate change and deforestation has the potential to alter the
96 exported terrigenous carbon fluxes as well as the amount of carbon that is exported to either
97 the atmosphere or the ocean tremendously. The local import of carbon to the river can act as
98 nutrient supply and therefore alters the habitat for plants and animals inhabiting the river,
99 while the regional export of carbon from the entire Amazon basin alters the amount of carbon
100 stored and therewith the carbon-sink potential of Amazonia (Hamilton, 2010).

101 The aim of our study is to elaborate on these combined effects of climate change and
102 deforestation on the riverine carbon fluxes, on the export of organic material into the Atlantic
103 Ocean and on the outgassing of riverine carbon to the atmosphere. **We believe that including**

104 the interaction between river and land to the assessment of future changes in the Amazon
105 basin is of importance to get a more complete view of how much the regional and global
106 carbon cycle might change.

107 To address these issues basin-wide data are needed, which not only describe the current
108 situation but also assess future developments. On-site measurements are limited to some
109 certain point in time and/or space. To partly overcome these limitations we make use of the
110 well-established dynamic global vegetation model LPJmL together with the riverine carbon
111 model RivCM. While LPJmL (Bondeau et al., 2007; Gerten et al., 2004; Rost et al., 2008;
112 Sitch et al., 2003) provides plausible estimates for the carbon and water pools and fluxes
113 within the coupled soil-vegetation system, RivCM (Langerwisch et al., 2015) focuses on the
114 export, conversion and transport of terrestrial fixed carbon in the river and to the atmosphere
115 and ocean. In Langerwisch et al. (2015) the solely effects of climate change have been
116 estimated. The results of the mentioned study show that climate change causes a doubling of
117 riverine organic carbon in the Southern and Western basin while reducing it by 20% in the
118 eastern and northern parts towards the end of the current century. In contrast, the amount of
119 riverine inorganic carbon shows a 2- to 3-fold increase in the entire basin, independent of the
120 SRES scenario. The export of carbon to the atmosphere increases as well with an average of
121 about 30%. The amount of organic carbon exported to the Atlantic Ocean depend on the
122 SRES scenario and are projected to either decrease by about 8.9% (SRES A1B) or increase by
123 about 9.1% (SRES A2). This current study, which is an extension of Langerwisch et al.
124 (2015) aims to investigate the combined effects of climate change and deforestation on the
125 riverine carbon. The coupled model LPJmL-RivCM was forced by several climate change and
126 deforestation scenarios that cover a wide range of uncertainties. We estimated temporal and
127 spatial changes in three riverine carbon pools as well as changes in the export of carbon to the
128 atmosphere and the ocean.

129 **2 Methods**

130 The impacts of climate change and deforestation on riverine carbon pools and fluxes in the
131 Amazonian watershed are assessed by the model RivCM (Langerwisch et al., 2015) for a
132 range of scenarios. RivCM is a grid-based model that assesses the transport and export of
133 carbon at monthly time steps and is driven climate data and terrestrial carbon pools. Climate
134 inputs are taken from different global climate model simulations driven by three SRES
135 scenarios (Nakićenović et al., 2000). Terrestrial carbon inputs are estimated by the process-
136 based dynamic global vegetation and hydrology model LPJmL (Bondeau et al., 2007; Gerten
137 et al., 2004; Rost et al., 2008; Sitch et al., 2003). To estimate soil and vegetation carbon,
138 LPJmL uses the above mentioned climate data and a set of deforestation scenarios from a
139 regional projections by SimAmazonia (Soares-Filho et al., 2006). An overview of the
140 interconnection between the two models and the scenarios is given in Figure 1.

141 **2.1 Model descriptions**

142 **2.1.1 LPJmL – a dynamic global vegetation and hydrology model**

143 The process-based global vegetation and hydrology model LPJmL (Bondeau et al., 2007;
144 Gerten et al., 2004; Rost et al., 2008; Sitch et al., 2003) calculates carbon and corresponding
145 water fluxes globally on a spatial resolution of 0.5×0.5 degree (lat/lon) in daily time steps.
146 For calculating the main processes, controlling the dynamics of potential natural vegetation
147 and thus carbon pools for vegetation, litter and soil, LPJmL uses climate data (temperature,
148 precipitation, and cloud cover), atmospheric CO₂ concentration, and soil type as input. The
149 main processes are photosynthesis, which is modelled according to Farquhar et al. (1980) and
150 Collatz et al. (1992), auto- and heterotrophic respiration, establishment, mortality, and
151 phenology. The simulated water fluxes include evaporation, soil moisture, snowmelt, runoff,
152 discharge, interception, and transpiration, which are directly linked to abiotic and biotic
153 properties. In each grid cell LPJmL calculates the performance of nine plant functional types,
154 which represent an assortment of species classified as being functionally similar. In the
155 Amazon basin primarily three of these types are present, namely tropical evergreen and
156 deciduous trees and C4 grasses. In addition to the potential natural vegetation LPJmL can
157 simulate the dynamics of 16 user-defined crops and pasture on area that is not covered by
158 natural vegetation. In analogy to natural vegetation, LPJmL evaluates carbon storage in
159 vegetation, litter and soil as well as water fluxes for these areas.

160 LPJmL has been shown to reproduce current patterns of biomass production (Cramer et al.,
161 2001; Sitch et al., 2003), carbon emission through fire (Thonicke et al., 2010), also including
162 managed land (Bondeau et al., 2007; Fader et al., 2010; Rost et al., 2008), and water dynamics
163 (Biemans et al., 2009; Gerten et al., 2004, 2008; Gordon et al., 2004; Wagner et al., 2003).
164 The simulated patterns in water fluxes, like evapotranspiration, runoff and soil moisture, are
165 comparable to stand-alone global hydrological models (Biemans et al., 2009; Gerten et al.,
166 2004; Wagner et al., 2003).

167 **2.1.2 RivCM – a riverine carbon model**

168 RivCM is a process-based model that calculates four major ecological processes related to the
169 carbon budget of the Amazon River (Figure 1B). These processes include (1) mobilization,
170 (2) decomposition and (3) respiration within the river, and (4) outgassing of CO₂ to the
171 atmosphere (Langerwisch et al., 2015). During mobilization parts of terrigenous litter and soil
172 carbon, as it is provided by LPJmL, is imported to the river, depending on inundated area. The
173 further processing of the terrigenous carbon in the river happens during its decomposition,
174 which represents the manual breakup, and its respiration, representing the biochemical
175 breakup. Finally the CO₂ that is produced during respiration can outgas if the saturation
176 concentration is exceeded (Langerwisch et al., 2015). These four processes directly control
177 the most relevant riverine carbon pools, namely particulate organic carbon (POC), dissolved
178 organic carbon (DOC), and inorganic carbon (IC), as well as outgassed atmospheric carbon
179 (representing CO₂), and exported riverine carbon to the ocean (either as POC, DOC, or IC).

180 The model is coupled to LPJmL by using the calculated monthly litter and soil carbon and
181 water amounts as inputs. It operates at the spatial resolution of 0.5×0.5 degree (lat/lon) and
182 on monthly time steps. The ability of the coupled model LPJmL-RivCM to reproduce current
183 conditions in riverine carbon concentration and export to either the atmosphere or the ocean
184 has been shown and discussed by Langerwisch et al. (2015). A validation of the carbon pools
185 and fluxes with observed data shows that RivCM produces results that are within the range of
186 observed concentrations of both organic and inorganic carbon pools, but it underestimates the
187 outgassed carbon strongly while it overestimates the carbon discharged to the ocean. Nevertheless
188 we are certain that relative changes in the carbon can be assessed by the model. Here, we
189 therefore use the coupled model to assess the combined impacts of climate change and
190 deforestation.

191 2.2 Model simulation

192 All transient LPJmL runs were preceded by a 1000-year spin-up during which the pre-
193 industrial CO₂ level of 280 ppm and the climate of the years 1901-1930 have been repeated to
194 obtain equilibria for vegetation, carbon, and water pools. All transient runs of the coupled
195 model LPJmL-RivCM have been preceded by a 90-years-spinup during which the climate and
196 CO₂ levels of 1901-1930 have been repeated to obtain equilibria for riverine carbon pools.

197 LPJmL-RivCM was run on a $0.5^\circ \times 0.5^\circ$ degree (lat/lon) spatial resolution for the years 1901
198 to 2099. For the estimation of the impact of projected climate change (CC) and deforestation
199 (Defor), simulations have been conducted driven by five General Circulation Models
200 (GCMs), each calculated for three SRES emission scenarios, and three LUC scenarios.

201 2.2.1 Climate change and deforestation data sets

202 To assess the effect of future climate change, projections of five GCMs (see also Jupp et al.,
203 2010; Randall et al., 2007), using three SRES scenarios (A1B, A2, B1) (Nakićenović et al.,
204 2000) have been applied (Figure 1A). The GCMs, namely MIUB-ECHO-G, MPI-ECHAM5,
205 MRI-CGCM2.3.2a, NCAR-CCSM3.0, UKMO-HadCM3, cover a wide range in terms of
206 temperature and precipitation and have therefore been chosen to account for uncertainty in
207 climate projections. The emission scenario SRES A1B describes a development of very rapid
208 economic growth with convergence among regions, and a balanced future energy source
209 between fossil and non-fossil. SRES A2 describes a development of a very heterogeneous
210 world with slow economic growth. And SRES B1 describes a development of converging
211 world similar to A1B but with more emphasis on service and information economy.

212 To estimate the additional effects of deforestation on riverine carbon pools and fluxes three
213 land use scenarios were applied: two scenarios directly relate to different intensity of
214 deforestation, and one represents a reference scenario with complete coverage by natural
215 vegetation (NatVeg scenario, hereafter). The two deforestation scenarios are based on the
216 SimAmazonia projections (Soares-Filho et al., 2006). The authors estimate the development
217 of deforestation in the Amazon basin until 2050 based on historical trends and projected
218 developments. In the business-as-usual scenario (BAU) they assume that recent deforestation
219 trends continue, the number of paved highways increases, and new protected areas are not

220 established. In contrast, deforestation is more efficiently controlled in the governance scenario
 221 (GOV). For this scenario the authors assume that the Brazilian environmental legislation is
 222 implemented across the Amazon basin and the size of the area under the *Protected Areas*
 223 *Program* increases. The SimAmazonia scenarios cover the years from 2001 to 2050. The
 224 period between 2051 and 2099 was further included into our study to show the long term
 225 effects of deforestation, while further deforestation is neglected over this period. In addition
 226 deforestation rates preceding the deforestation scenarios were derived from extrapolating the
 227 data into the past. LPJmL requires historic land-cover information to correctly capture
 228 transient carbon dynamics. The model starts to simulate vegetation dynamics from bare
 229 ground and can't be initialized with a land-cover map of a particulate year. It was therefore
 230 necessary to develop an approach which produced consistent land-cover information for the
 231 (undisturbed) past and the deforestation scenarios. For that, the mean annual rate of
 232 deforestation was calculated for the reference period of 2001 to 2005 (Eq. (1)) and this rate
 233 was applied to calculate the fraction of deforested area F_t for the years 1901 to 2000 for each
 234 cell (Eq. (2)).

$$r = \left(\sum_{t=2001}^{2005} \frac{F_t}{F_{t+1}} \right) \times \frac{1}{2006 - 2001} \quad (1)$$

$$F_t = F_{2001} \times r^{2001-t} \quad (2)$$

235

236 To evaluated special differences in the basin we defined three sub-regions (see Table 1).
 237 Three regions were selected for further detailed analysis. R1 is located in the Western basin
 238 with projected increase in inundation length and inundated area (Langerwisch et al., 2013)
 239 combined with low land use intensity. R2 is a region covering the Amazon main stem with
 240 intermediate changes in inundation (Langerwisch et al., 2013) and intermediate land use
 241 intensity. And R3 is a region with projected decrease in duration of inundation and inundated
 242 area (Langerwisch et al., 2013) combined with high land use intensity. In the deforestation
 243 scenarios we assume that on 15% of the deforested area soy bean is grown and 85% of the
 244 area is used as pasture for beef production (Costa et al., 2007).

245 **2.3 Analysis of simulation results**

246 The net effect of deforestation (E_{Defor}) is estimated by calculating the differences between
 247 future carbon amounts (2070-2099) produced in the deforestation scenarios (GOV or BAU)
 248 and future carbon amounts produced in the potential natural vegetation scenario (NatVeg),
 249 where no deforestation is assumed. The combined effect of climate change and deforestation
 250 ($E_{CCDefor}$) is estimated by calculating the differences between future carbon amounts produced
 251 in the deforestation scenarios and reference carbon amounts (1971-2000) produced in the
 252 NatVeg scenario. Carbon can occur in the river either in an organic or inorganic form.
 253 Therefore the following four different carbon pools have been analysed: the riverine
 254 particulate organic carbon (POC) and dissolved organic carbon (DOC), as well as the riverine
 255 inorganic carbon pool (IC) and outgassed carbon. The relative changes in POC and DOC

256 show similar patterns (see Fig. S1), therefore exemplary POC is shown and discussed in
 257 detail.

258 **2.3.1 Evaluation of potential future changes**

259 Spatial effects of the two deforestation scenarios (GOV and BAU) on the different riverine
 260 carbon pools and fluxes have been estimated by calculating the common logarithm (\log_{10}) of
 261 the ratio of mean future (2070-2099) carbon amounts of the deforestation scenarios and mean
 262 future carbon amounts of the NatVeg scenario (E_{Defor} , Eq. (3)) for each simulation run.

$$E_{Defor} = \log_{10} \frac{\sum_{t=2070}^{2099} C_{Defor_t}}{\sum_{t=2070}^{2099} C_{NatVeg_t}} \quad (3)$$

263 To estimate changes caused by the combination of climate change and deforestation $E_{CCDefor}$
 264 compares future carbon pools in the deforestation scenarios to carbon pools during the
 265 reference period (1971-2000) in the NatVeg scenario (Eq. (4)).

$$E_{CCDefor} = \log_{10} \frac{\sum_{t1=2070}^{2099} C_{Defor_{t1}}}{\sum_{t2=1971}^{2000} C_{NatVeg_{t2}}} \quad (4)$$

266 Each simulation run combines deforestation and emission scenarios and aggregates the
 267 outputs for all five climate model inputs used. To identify areas where the differences
 268 between values in the reference period and future values are significant (p-value <0.05), the
 269 Wilcoxon Rank Sum Test for not-normally distributed datasets (Bauer, 1972) has been
 270 applied for each cell.

271 Additionally to the spatial assessment, time series were deduced based on mean values over
 272 the entire basin and each of the three exemplary regions R1, R2 and R3. These means of the
 273 carbon pools were calculated for every year during the simulation period. Changes have been
 274 expressed as the five-year-running-mean of the quotient of annual future carbon amounts in
 275 the deforestation and in the NatVeg scenarios. These analyses have been conducted both for
 276 the whole Amazon basin and for three selected sub-regions.

277 **2.3.2 Estimating the dominant driver for changes**

278 We estimated which factor is causing the observed changes the most. To estimate the
 279 contribution of either climate change (D_{CC} , Eq. (5)) or deforestation (D_{Defor} , Eq. (6)),
 280 reference carbon amounts of the NatVeg scenario have been compared to future amounts of
 281 the NatVeg scenario (D_{CC}), and future carbon amounts of the NatVeg scenario have been
 282 compared to future amounts of the deforestation scenarios (D_{Defor}).

$$D_{CC} = \left| \log_{10} \frac{\sum_{t1=2070}^{2099} C_{NatVeg_{t1}}}{\sum_{t2=1971}^{2000} C_{NatVeg_{t2}}} \right| \quad (5)$$

$$D_{Defor} = |E_{Defor}| \quad (6)$$

283 We define a cell as dominated by climate change effects, if $D_{CC} > D_{Defor}$ and dominated by
284 deforestation effects if $D_{CC} < D_{Defor}$. The impact values D_{CC} and D_{Defor} ($median_{POC} = 0.9695$,
285 $median_{IC} = 1.0106$, and $median_{outgassedC} = 0.9982$) have been rounded to the second decimal
286 place. If both values are equal, the two effects balance each other.

287

288 3 Results

289 3.1 Changes caused by deforestation

290 Deforestation leads to a decrease in riverine particulate and dissolved organic carbon (POC
291 and DOC). **Figure 2A** and **Figure 2B** show that the decrease is more intense under the BAU
292 than under the GOV scenario (for DOC see Figs. S1A and S1B). In some highly deforested
293 sites the POC amount is only 10% of the amount under no deforestation (indicated by E_{Defor}).
294 This pattern is robust between the model realizations with a high agreement of the results
295 amongst the five climate models. Compared to the deforestation scenarios the differences
296 between the three emission scenarios (A1B, A2, and B1) are very small, i.e. even under the
297 moderate emission scenario B1 the decrease in POC can be drastic. Despite the overall
298 decrease there are few areas where POC increases (up to 3fold), especially in mountain
299 regions (e.g. Andes and Guiana Shield). DOC and POC follow the same spatial and temporal
300 patterns in change (see Fig. S1) therefore only one of the carbon pools, namely POC, is shown
301 and discussed in detail. Although POC and DOC respond similar in relative terms, the
302 absolute amounts are approximately twice as high for DOC compared to POC (Table 2). The
303 mean basin-wide loss in POC ranges between $0.13 \times 10^{12} \text{ g yr}^{-1}$ (A2) and 0.24 (A1B)
304 $\times 10^{12} \text{ g yr}^{-1}$ (A1B) in the GOV scenario, and between $0.37 \times 10^{12} \text{ g yr}^{-1}$ (A2) and
305 $0.48 \times 10^{12} \text{ g yr}^{-1}$ (A1B) in the BAU scenario. As with the relative changes the absolute
306 differences show that compared to the deforestation scenarios the effect of the different
307 emission scenarios on POC and DOC is small. The SRES A2 scenario causes the largest
308 changes, further increasing the loss caused by land use change.

309 Changes in outgassed riverine carbon caused by deforestation (**Figure 2C** and **Figure 2D**)
310 show a similar pattern as the changes in POC, with an even clearer effect of deforestation on a
311 larger area. In both scenarios deforestation leads to a decrease in outgassed carbon to up to a
312 tenth compared to the amount produced under the NatVeg scenario. The agreement between
313 the five climate models is even larger than in POC. Some areas in the Andes and the Guiana
314 Shield show an increase in outgassed carbon of up to a factor of 30, but these areas are an
315 exception. Like in POC the differences between the SRES scenarios are only minor. For the
316 absolute values see Table 2.

317 For riverine inorganic carbon (IC) deforestation caused significant changes (E_{Defor} , p-value
318 < 0.05) only in small areas (**Figure 2E** and **Figure 2F**). In these regions, in the very South of
319 the basin and in single spots in the North, i.e. in the headwaters of the watershed, IC increases
320 by a factor of up to 1.2. Besides these areas of increase, a slight decrease of about 5% is
321 simulated for the region along the main stem of the Amazon River, downstream of Manaus

322 and along the Rio Madeira and the Rio Tapajós. In contrast to POC, the spatial pattern of
323 change in IC does not obviously follow the deforestation patterns. Therefore, the differences
324 between the two deforestation scenarios GOV and BAU scenarios are minor. Whereas POC,
325 DOC, and outgassed carbon show a clear decrease due to deforestation, IC shows a nearly
326 neutral response with maximal mean basin-wide gains (for absolute values see Table 2).

327 **3.2 Changes caused by a combination of deforestation and climate change**

328 Climate change and deforestation together will lead to large overall changes in the amount of
329 riverine and exported carbon. Riverine POC and DOC amounts will decrease by about 19.8%
330 and 22.2%, respectively, and exported organic carbon will decrease by about 38.1% (Figure
331 3). In contrast riverine IC will increase by about 100%, combined with a slight increase of
332 outgassed carbon by about 2.7% (Figure 3). In detail, the basin-wide changes in the amount of
333 POC (Figure 4A-B and Figure 5A) caused by deforestation and climate change range between
334 a 2.5-fold increase and a decrease to one tenth. The increase is mainly caused by climate
335 change (indicated by the green cell borders in Figure 4), whereas the decrease is mainly
336 caused by deforestation (red cell borders). The differences mainly induced by deforestation
337 are larger in the BAU compared to the GOV scenario. In contrast, the differences caused by
338 climate change show no large differences between the two deforestation scenarios. The
339 differences between the emission scenarios are minor (see also Table 2). In some areas the
340 dominance of forcing shifts from climate change dominance (D_{CC}) for the GOV scenario
341 (green cell border) to deforestation dominance (D_{Defor}) for the BAU scenario (red cell border)
342 due to the higher land use intensity as a result of deforestation (see also Table 3). While in the
343 GOV scenario 20% of all cells are dominated by deforestation impacts, this value increases
344 for the BAU scenario to 30%. During the first decades (2000-2030) basin-wide POC is partly
345 larger in the deforestation scenarios than in the NatVeg scenario by up to 2% in 2000 and
346 about 1% in 2020 (Figure 5A). All climate models show reduced POC amounts in the
347 deforestation scenarios compared to the NatVeg scenario after 2040. The POC amount in the
348 GOV deforestation scenario decreases gradually until the decrease levels off in the late 2060s,
349 i.e. ten years after the constant deforestation area is kept constant. In the BAU scenario, POC
350 decreases strongly in the 2040 to 2060s leading to a loss of about 25% compared to 10% in
351 the GOV scenario. The three sub-regions R1 to R3 show different patterns (Figure 5A). While
352 in region R1 the difference in the POC amounts between the GOV and the BAU scenario is
353 only small, reflecting the low deforestation in this region, the differences between the two
354 deforestation scenarios are more explicit in regions R2 and especially in R3 (with the largest
355 area deforested), where in addition model uncertainty is low. Starting in the 2050s, the
356 variation between different emission scenarios and climate models increases. Alike the results
357 of the impact of deforestation alone POC and DOC show a similar pattern. Therefore only
358 results for POC are shown and explained in detail (see also Table 2).

359 The changes in outgassed carbon (Figure 4C-D and Figure 5B) are in the same range as
360 changes in POC. The large-scale gain in outgassed carbon of about 20%, especially in the
361 North-Western basin, is driven by climate change (Figure 4C-D). The deforestation induces a
362 decrease to one tenth in areas with high fraction of deforested area, i.e. in the Eastern and
363 South-Eastern basin. The effect of the two deforestation scenarios (GOV vs. BAU) is much

364 larger than the effect of the different emission scenarios (see also Table 2). Temporarily the
365 differences in the amount of outgassed carbon (Figure 5B) show a strong deforestation-driven
366 pattern as well. The outgassed carbon directly depends on the available POC, therefore the
367 time series of both, POC and IC widely match. In the GOV scenario the basin-wide loss of
368 outgassed carbon is about 16% towards the end of the century. The results of the BAU
369 scenario show an average loss of outgassed carbon of 28%.

370 Changes in inorganic carbon (IC) are mainly caused by climate change for both deforestation
371 scenarios and all emission scenarios (Figure 4E-F and Figure 5C, Tables 2 and 3). The IC
372 amount significantly changes in about 50% of the cells due to climate change and in no cell
373 due to land use change. The magnitude of change varies between emission scenarios: the
374 increase in IC is up to 4-fold in the A2 scenario and up to 2.5-fold in the B1 scenario (see
375 Table 2). For both deforestation scenarios the gain of IC is dominant until 2050, while the
376 basin-wide trend becomes unclear afterwards. However, sub-regions like R1 and R3 show a
377 slight increase during the whole century (Figure 5C).

378

379 **4 Discussion**

380 Deforestation is, besides climate change, the largest threat to Amazonia. It leads directly to a
381 decrease in terrestrial biomass and an increase in CO₂ emissions (Potter et al., 2009) and has
382 indirect effects on aquatic biomass, diversity of species and biotopes and the climate (Asner
383 and Alencar, 2010; Bernardes et al., 2004; Costa et al., 2003).

384 **4.1 Temporal trends in carbon pools**

385 Our results show that deforestation leads to a basin-wide reduction in riverine particulate and
386 dissolved organic carbon pools by the end of the century by about 10% to 25% (Figure 5).
387 This reduction is particularly pronounced in areas of high deforestation intensity at the *Arc of*
388 *Deforestation*, at the Rio Madeira and the last 500 km stretch of the Rio Amazon. In the first
389 decades of the 21st century the differences in carbon amounts between the two land use
390 intensities are only small (Figure 5). During these decades in both scenarios a deforestation
391 induced increase in discharge (as reported by Costa et al., 2003), is able to balance the
392 decreasing amount of terrigenous organic matter which is the source of riverine organic
393 matter. The differences in the organic carbon pools caused by deforestation become more
394 obvious after the 2050s (Figure 5), with larger carbon decrease in the more severe BAU
395 scenario. After 2050 the deforested area remains constant and the variation within the results
396 can be attributed to the climate models and emission scenarios.

397 **4.2 Shortcomings of the deforestation scenarios and implementation of crops in** 398 **LPJmL**

399 The strong decrease of organic carbon is especially pronounced because we assume a
400 complete removal of the natural vegetation carbon during deforestation (see e.g. Figure 5). In
401 reality, the complete conversion of the floodplain forests to cropland or pasture is not very

402 likely. In the more severe deforestation scenario (BAU) about 6% of the area is deforested
403 (Soares-Filho et al., 2006). In our scenarios this also includes areas which are temporarily
404 flooded. This might sound unrealistic, since temporarily inundated areas cannot be easily
405 converted to agricultural area or settlements. But on the other hand in Manaus, floodplains
406 within a radius of about 500 km around the city have been extensively logged for construction
407 purposes between 1960 and 1980 (Goulding et al., 2003).

408 In our study deforestation is simulated by partial or complete removal of vegetation carbon.
409 This also reduces the litter and soil carbon through respiration over time in these areas,
410 because these pools are not refilled by litter fall from the vegetation. Because the deforested
411 cell fraction has been kept constant from 2050 to 2099 the results show how carbon pools
412 stabilize after 2050. The clear decrease in POC and outgassed carbon after 2050 as it is one
413 result of our study is caused by the implementation of carbon removal in the model. During
414 inundation the cells are partly or completely covered with water, which leads to the export of
415 organic material. After the gradual decrease of forest cover (and therewith input of organic
416 material) before 2050, there is a depletion of the remaining organic material in the following
417 years. By a more gradual implementation of inundation in the model this harsh decrease
418 would be softened.

419

420 **4.3 Consequences of the changed riverine carbon pools**

421 The reduction in the riverine organic carbon pools, which is caused by extensive
422 deforestation, will have consequences for the floodplain and the river itself. Floodplains as
423 well as riverine biotopes depend on the annually recurring input of organic material, either as
424 food supply or fertilizer (Junk and Wantzen, 2004). The productivity of the floodplain forests
425 is mainly driven by the input of nutrients which are basically sediments and organic material
426 (Worbes, 1997). While the sediment input bringing new nutrients might increase due to
427 increased discharge, the input of organic material from upstream areas will decrease, leading
428 to a reduced productivity. This reduced productivity will certainly impact many animal
429 species that rely on the food supplied by the trees, like fruits or leaves. The reduced supply
430 with fertilizer and food will therefore affect plant and animal species compositions on local and
431 regional scales (Junk and Wantzen, 2004; Worbes, 1997).

432 Additionally, deforestation will have secondary effects, including a reduction in evasion of
433 CO₂ from the water (outgassed carbon). Lower terrestrial productivity after deforestation
434 decreases the organic carbon material in the river and thus also the respiration to CO₂. This is
435 opposed by the higher respiration rate as a result of increased temperatures as part of the
436 projected climate change. In addition, both, the higher water temperature, causing a reduction
437 in solubility of CO₂, and a higher atmospheric CO₂ concentration, lead in combination to a
438 slight increase in dissolved inorganic carbon in the beginning and a neutral signal towards the
439 end of the century.

440 In the presented study the mobilization of terrigenous organic material is exclusively
441 controlled by inundation. A model that also considers the impact of precipitation, vegetation
442 cover and slope on erosion would likely lead to an increase in erosion and thus to the import

443 of organic matter to the river (McClain and Elsenbeer, 2001) in the first years after
444 deforestation. However, this additional influx of carbon would only be temporal, since the soil
445 and litter carbon pools would be eroded after some years (McClain and Elsenbeer, 2001).
446 Thus, we assume that for the investigation of the long-term dynamics of carbon pools and
447 fluxes, such erosion effects are only of minor importance.

448 **4.4 Consequences of the changed carbon export from the basin**

449 The deforestation of rainforest will not only affect processes within the rainforest, but also
450 processes in the adjacent Atlantic Ocean. Currently, the annual export of about 6,300 km³ of
451 freshwater is accompanied by 40×10¹² g of organic carbon to the Atlantic Ocean (Gaillardet et
452 al., 1997; Moreira-Turcq et al., 2003). The present study shows that deforestation leads to a
453 reduction in the exported organic carbon to the ocean by approximately 40%. In the NatVeg
454 scenario the proportion of exported organic carbon to the ocean makes up about 0.8-0.9% of
455 the net primary productions (NPP), whereas in the heavily deforested BAU scenario this
456 proportion is reduced to about 0.5-0.6%. The reduction in the ratio of exported carbon to NPP
457 by deforestation indicates a less pronounced future sink, since the organic carbon is directly
458 extracted from the forest and additionally indirectly from the ocean. Globally about
459 120×10¹⁵g carbon per year are fixed by the terrestrial vegetation during GPP. After
460 autotrophic and heterotrophic respiration about 1×10¹⁵ g carbon per year are fixed in new
461 biomass (NEP). To assess the future potential of one of the largest tropical forests, the
462 Amazon basin, to act as a carbon sink to the atmosphere has to include therefore the loss of
463 carbon to the ocean to have a more complete view on the global carbon cycle.

464 The import of organic material to the ocean positively impacts the respiration and production
465 of the Atlantic Ocean off the coast of South America (Körtzinger, 2003; Cooley and Yager,
466 2006; Cooley et al., 2007; Subramaniam et al., 2008). A reduction of the import might
467 therefore reduce the productivity in the coast-near ocean since these depend on the imported
468 organic matter (Cooley and Yager, 2006; Körtzinger, 2003; Subramaniam et al., 2008) and
469 might have further impacts along the trophic cascade including herbivorous and piscivorous
470 fish. Besides the reduced organic carbon, there might be an elevated amount of nutrients,
471 which are only marginally taken up within the river and by the former intact adjacent forests.
472 The imports of both, less organic carbon and more nutrients, might induce changes in oceanic
473 heterotrophy and primary production.

474 **4.5 Conclusion**

475 Deforestation is associated with a decrease in terrestrial biomass and an increase in CO₂
476 emissions, which leads to a reduction in the terrestrial sequestration potential (Houghton et
477 al., 2000; Potter et al., 2009). On top, our results show that deforestation will lead to a
478 significant decrease of exported terrigenous organic carbon, leading to a reduction in riverine
479 organic carbon. The climate change effects, such as increased atmospheric CO₂ concentration,
480 lead to an increase in riverine inorganic carbon. Climate change alone will lead to an increase
481 in riverine organic carbon of about 10%, almost no changes in export to the Atlantic Ocean,
482 and a drastic increase in outgassed carbon of about 40% (Langerwisch et al., 2015). In
483 combination with deforestation riverine organic carbon will decrease by about 20%, export of

484 organic carbon to the ocean will decrease by about 40%, while outgassed carbon slightly
485 increases.

486 These changes in the hydrological regimes and the fluvial carbon pools might add to the
487 pressures that are being encountered in the Amazon ecosystems (Asner et al., 2006; Asner and
488 Alencar, 2010) and its consequences on ecosystem stability (Brown and Lugo, 1990; Foley et
489 al., 2002; von Randow et al., 2004). For instance, fish play a key role in seed dispersal in
490 along the Amazon, and if floodplains turn less productive ground for juvenile fish, these
491 changes might affect even vegetation composition (Horn et al. 2011). We therefore strongly
492 advocate the combined terrestrial and fluvial perspective of our approach, and its ability to
493 address both climate and land use change.

494

495

496 *Acknowledgements.* We thank “Pakt für Forschung der Leibniz-Gemeinschaft” for funding the
497 TRACES project for FL. AR was funded by FP7 AMAZALERT (Project ID 282664) and
498 Helmholtz Alliance ‘Remote Sensing and Earth System Dynamics’. We also thank Susanne
499 Rolinski and Dieter Gerten for discussing the hydrological aspects. We thank Alice Boit for
500 fruitful comments on the manuscript. Additionally we thank our LPJmL and ECOSTAB
501 colleagues at PIK for helpful comments on the design of the study and the manuscript.

502 *Author contributions.* Model development: FL, BT, WC. Data analysis: FL, AR, KT. Drafting
503 the article: FL, AW, BT, AR, KT.

504

505 **5 References**

506 Anderson, J. T., Nuttle, T., Saldaña Rojas, J. S., Pendergast, T. H. and Flecker, A. S.:
507 Extremely long-distance seed dispersal by an overfished Amazonian frugivore, *Proceedings*
508 *of the Royal Society B: Biological Sciences*, 278, 3329–3335, doi:10.1098/rspb.2011.0155,
509 2011.

510 Asner, G. P. and Alencar, A.: Drought impacts on the Amazon forest: the remote sensing
511 perspective, *New Phytologist*, 187(3), 569–578, doi:10.1111/j.1469-8137.2010.03310.x,
512 2010.

513 Asner, G. P., Broadbent, E. N., Oliveira, P. J. C., Keller, M., Knapp, D. E. and Silva, J. N. M.:
514 Condition and fate of logged forests in the Brazilian Amazon, *Proceedings of the National*
515 *Academy of Sciences*, 103(34), 12947–12950, 2006.

516 Bauer, D. F.: Constructing confidence sets using rank statistics, *Journal of the American*
517 *Statistical Association*, 67(339), 687–690, 1972.

518 Bernardes, M. C., Martinelli, L. A., Krusche, A. V., Gudeman, J., Moreira, M., Victoria, R.
519 L., Ometto, J. P. H. B., Ballester, M. V. R., Aufdenkampe, A. K., Richey, J. E. and Hedges, J.

- 520 I.: Riverine organic matter composition as a function of land use changes, Southwest
521 Amazon, *Ecological Applications*, 14(4), S263–S279, doi:10.1890/01-6028, 2004.
- 522 Biemans, H., Hutjes, R. W. A., Kabat, P., Strengers, B. J., Gerten, D. and Rost, S.: Effects of
523 precipitation uncertainty on discharge calculations for main river basins, *Journal of*
524 *Hydrometeorology*, 10(4), 1011–1025, doi:10.1175/2008jhm1067.1, 2009.
- 525 Bondeau, A., Smith, P. C., Zaehle, S., Schaphoff, S., Lucht, W., Cramer, W., Gerten, D.,
526 Lotze-Campen, H., Müller, C., Reichstein, M. and Smith, B.: Modelling the role of agriculture
527 for the 20th century global terrestrial carbon balance, *Global Change Biology*, 13(3), 679–
528 706, doi:10.1111/j.1365-2486.2006.01305.x, 2007.
- 529 Brown, S. and Lugo, A. E.: Tropical secondary forests, *Journal of Tropical Ecology*, 6(1), 1–
530 32, 1990.
- 531 Collatz, G. J., Ribas-Carbo, M. and Berry, J. A.: Coupled photosynthesis-stomatal
532 conductance model for leaves of C4 plants, *Functional Plant Biology*, 19(5), 519–538,
533 doi:10.1071/PP9920519, 1992.
- 534 Cooley, S. R. and Yager, P. L.: Physical and biological contributions to the western tropical
535 North Atlantic Ocean carbon sink formed by the Amazon River plume, *Journal of*
536 *Geophysical Research-Oceans*, 111(C08018), doi:10.1029/2005JC002954, 2006.
- 537 Cooley, S. R., Coles, V. J., Subramaniam, A. and Yager, P. L.: Seasonal variations in the
538 Amazon plume-related atmospheric carbon sink, *Global Biogeochemical Cycles*, 21(3),
539 doi:10.1029/2006GB002831, 2007.
- 540 Costa, M. H., Botta, A. and Cardille, J. A.: Effects of large-scale changes in land cover on the
541 discharge of the Tocantins River, Southeastern Amazonia, *Journal of Hydrology*, 283(1-4),
542 206–217, doi:10.1016/S0022-1694(03)00267-1, 2003.
- 543 Costa, M. H., Yanagi, S. N. M., Souza, P., Ribeiro, A. and Rocha, E. J. P.: Climate change in
544 Amazonia caused by soybean cropland expansion, as compared to caused by pastureland
545 expansion, *Geophysical Research Letters*, 34(7), doi:L07706 Artn I07706, 2007.
- 546 Cramer, W., Bondeau, A., Woodward, F. I., Prentice, I. C., Betts, R. A., Brovkin, V., Cox, P.
547 M., Fisher, V., Foley, J. A., Friend, A. D., Kucharik, C., Lomas, M. R., Ramankutty, N.,
548 Sitch, S., Smith, B., White, A. and Young-Molling, C.: Global response of terrestrial
549 ecosystem structure and function to CO₂ and climate change: results from six dynamic global
550 vegetation models, *Global Change Biology*, 7(4), 357–373, 2001.
- 551 Eva, H. D., Belward, A. S., De Miranda, E. E., Di Bella, C. M., Gond, V., Huber, O., Jones,
552 S., Sgrenzaroli, M. and Fritz, S.: A land cover map of South America, *Global Change*
553 *Biology*, 10(5), 731–744, 2004.
- 554 Fader, M., Rost, S., Müller, C., Bondeau, A. and Gerten, D.: Virtual water content of
555 temperate cereals and maize: Present and potential future patterns, *Journal of Hydrology*,
556 384(3-4), 218–231, doi:10.1016/j.jhydrol.2009.12.011, 2010.
- 557 Farquhar, G. D., van Caemmerer, S. and Berry, J. A.: A biochemical model of photosynthetic
558 CO₂ assimilation in leaves of C3 species, *Planta*, 149, 78–90, 1980.

- 559 Foley, J. A., Botta, A., Coe, M. T. and Costa, M. H.: El Niño-Southern Oscillation and the
560 climate, ecosystems and rivers of Amazonia, *Global Biogeochemical Cycles*, 16(4), 79/1–
561 79/17, doi:10.1029/2002GB001872, 2002.
- 562 Foley, J. A., Asner, G. P., Costa, M. H., Coe, M. T., DeFries, R., Gibbs, H. K., Howard, E. A.,
563 Olson, S., Patz, J., Ramankutty, N. and Snyder, P.: Amazonia revealed: forest degradation and
564 loss of ecosystem goods and services in the Amazon Basin, *Frontiers in Ecology and the*
565 *Environment*, 5(1), 25–32, doi:10.1890/1540-9295(2007)5[25:ARFDAL]2.0.CO;2, 2007.
- 566 Gaillardet, J., Dupré, B., Allègre, C. J. and Négrel, P.: Chemical and physical denudation in
567 the Amazon River basin, *Chemical Geology*, 142(3-4), 141–173, 1997.
- 568 Gerten, D., Schaphoff, S., Haberlandt, U., Lucht, W. and Sitch, S.: Terrestrial vegetation and
569 water balance - hydrological evaluation of a dynamic global vegetation model, *Journal of*
570 *Hydrology*, 286(1-4), 249–270, doi:10.1016/j.jhydrol.2003.09.029, 2004.
- 571 Gerten, D., Rost, S., von Bloh, W. and Lucht, W.: Causes of change in 20th century global
572 river discharge, *Geophysical Research Letters*, 35(20), doi:L20405 10.1029/2008gl035258,
573 2008.
- 574 Godar, J., Gardner, T. A., Tizado, E. J. and Pacheco, P.: Actor-specific contributions to the
575 deforestation slowdown in the Brazilian Amazon, *Proceedings of the National Academy of*
576 *Sciences*, 111(43), 15591–15596, doi:10.1073/pnas.1322825111, 2014.
- 577 Gordon, W. S., Famiglietti, J. S., Fowler, N. L., Kittel, T. G. F. and Hibbard, K. A.:
578 Validation of simulated runoff from six terrestrial ecosystem models: results from VEMAP,
579 *Ecological Applications*, 14(2), 527–545, doi:10.1890/02-5287, 2004.
- 580 Goulding, M., Barthem, R. and Ferreira, E.: *The Smithsonian Atlas of the Amazon*,
581 Washington and London., 2003.
- 582 Hamilton, S. K.: Biogeochemical implications of climate change for tropical rivers and
583 floodplains, *Hydrobiologia*, 657(1), 19–35, doi:10.1007/s10750-009-0086-1, 2010.
- 584 Hedges, J. I., Mayorga, E., Tsamakidis, E., McClain, M. E., Aufdenkampe, A., Quay, P.,
585 Richey, J. E., Benner, R., Opsahl, S., Black, B., Pimentel, T., Quintanilla, J. and Maurice, L.:
586 Organic matter in Bolivian tributaries of the Amazon River: A comparison to the lower
587 mainstream, *Limnology and Oceanography*, 45(7), 1449–1466, 2000.
- 588 Hoorn, C., Wesselingh, F. P., Steege, H. ter, Bermudez, M. A., Mora, A., Sevink, J.,
589 Sanmartin, I., Sanchez-Meseguer, A., Anderson, C. L., Figueiredo, J. P., Jaramillo, C., Riff,
590 D., Negri, F. R., Hooghiemstra, H., Lundberg, J., Stadler, T., Sarkinen, T. and Antonelli, A.:
591 Amazonia through time: Andean uplift, climate change, landscape evolution, and biodiversity,
592 *Science*, 330(6006), 927–931, doi:10.1126/science.1194585, 2010.
- 593 Horn, M. H., Correa, S. B., Parolin, P., Pollux, B. J. A., Anderson, J. T., Lucas, C., Widmann,
594 P., Tjiu, A., Galetti, M. and Goulding, M.: Seed dispersal by fishes in tropical and temperate
595 fresh waters: The growing evidence, *Acta Oecologica*, 37, 561–577,
596 doi:10.1016/j.actao.2011.06.004, 2011.
- 597 Houghton, R. A., Skole, D. L., Nobre, C. A., Hackler, J. L., Lawrence, K. T. and
598 Chomentowski, W. H.: Annual fluxes of carbon from deforestation and regrowth in the
599 Brazilian Amazon, *Nature*, 403(6767), 301–304, 2000.

- 600 INPE: Projeto PRODES: Monitoramento da floresta Amazônica Brasileira por satélite.
601 [online] Available from: <http://www.obt.inpe.br/prodes/index.php> (Accessed 28 April 2015),
602 2013.
- 603 Irmler, U.: Litterfall and nitrogen turnover in an Amazonian blackwater inundation forest,
604 *Plant and Soil*, 67(1-3), 355–358, 1982.
- 605 Johnson, M. S., Lehmann, J., Selva, E. C., Abdo, M., Riha, S. and Couto, E. G.: Organic
606 carbon fluxes within and streamwater exports from headwater catchments in the southern
607 Amazon, *Hydrological Processes*, 20(12), 2599–2614, 2006.
- 608 Junk, W. J.: *The central Amazon floodplain - Ecology of a pulsing system*, Springer., 1997.
- 609 Junk, W. J. and Wantzen, K. M.: The flood pulse concept: New aspects, approaches and
610 applications - An update, in *Proceedings of the Second International Symposium on the*
611 *Management of large Rivers for Fisheries*, edited by R. L. Welcomme and T. Petr, pp. 117–
612 140., 2004.
- 613 Jupp, T. E., Cox, P. M., Rammig, A., Thonicke, K., Lucht, W. and Cramer, W.: Development
614 of probability density functions for future South American rainfall, *New Phytologist*, 187,
615 682–693, doi:10.1111/j.1469-8137.2010.03368.x, 2010.
- 616 Keller, M., Bustamante, M., Gash, J. and Silva Dias, P., Eds.: *Amazonia and global change*,
617 American Geophysical Union, Washington, DC., 2009.
- 618 Körtzinger, A.: A significant CO₂ sink in the tropical Atlantic Ocean associated with the
619 Amazon River plume, *Geophysical Research Letters*, 30(24), doi:10.1029/2003GL018841,
620 2003.
- 621 Langerwisch, F., Rost, S., Gerten, D., Poulter, B., Rammig, A. and Cramer, W.: Potential
622 effects of climate change on inundation patterns in the Amazon Basin, *Hydrology and Earth*
623 *System Sciences*, 17(6), 2247–2262, doi:10.5194/hess-17-2247-2013, 2013.
- 624 Langerwisch, F., Walz, A., Rammig, A., Tietjen, B., Thonicke, K. and Cramer, W.: Climate
625 change increases riverine carbon outgassing while export to the ocean remains uncertain,
626 *Earth System Dynamics Discussions*, 6(2), 1445–1497, doi:10.5194/esdd-6-1445-2015, 2015.
- 627 Lawrence, D. and Vandecar, K.: Effects of tropical deforestation on climate and agriculture,
628 *Nature Climate Change*, 5(1), 27–36, doi:10.1038/nclimate2430, 2014.
- 629 Malhi, Y., Wood, D., Baker, T. R., Wright, J., Phillips, O. L., Cochrane, T., Meir, P., Chave,
630 J., Almeida, S., Arroyo, L., Higuchi, N., Killeen, T. J., Laurance, S. G., Laurance, W. F.,
631 Lewis, S. L., Monteagudo, A., Neill, D. A., Vargas, P. N., Pitman, N. C. A., Quesada, C. A.,
632 Salomão, R., Silva, J. N. M., Lezama, A. T., Terborgh, J., Martínez, R. V. and Vinceti, B.:
633 The regional variation of aboveground live biomass in old-growth Amazonian forests, *Global*
634 *Change Biology*, 12(7), 1107–1138, 2006.
- 635 Malhi, Y., Roberts, J. T., Betts, R. A., Killeen, T. J., Li, W. and Nobre, C. A.: Climate change,
636 deforestation, and the fate of the Amazon, *Science*, 319(5860), 169–172, 2008.
- 637 Mayorga, E., Aufdenkampe, A. K., Masiello, C. A., Krusche, A. V., Hedges, J. I., Quay, P.
638 D., Richey, J. E. and Brown, T. A.: Young organic matter as a source of carbon dioxide

- 639 outgassing from Amazonian rivers, *Nature*, 436(7050), 538–541, doi:10.1038/nature03880,
640 2005.
- 641 McClain, M. E. and Elsenbeer, H.: Terrestrial inputs to Amazon streams and internal
642 biogeochemical processing, in *The Biogeochemistry of the Amazon Basin*, edited by M. E.
643 McClain, R. L. Victoria, and J. E. Richey, pp. 185–208, Oxford University Press, New York.,
644 2001.
- 645 Medeiros, P. M., Seidel, M., Ward, N. D., Carpenter, E. J., Gomes, H. R., Niggemann, J.,
646 Krusche, A. V., Richey, J. E., Yager, P. L. and Dittmar, T.: Fate of the Amazon River
647 dissolved organic matter in the tropical Atlantic Ocean, *Global Biogeochemical Cycles*, 29(5),
648 677–690, doi:10.1002/2015GB005115, 2015.
- 649 Melack, J. M. and Forsberg, B.: Biogeochemistry of Amazon floodplain lakes and associated
650 wetlands, in *The Biogeochemistry of the Amazon Basin and its Role in a Changing World*,
651 pp. 235–276, Oxford University Press, Eds. McClain, M. E.; Victoria, R. L.; Richey, J. E.,
652 2001.
- 653 Moreira-Turcq, P., Seyler, P., Guyot, J. L. and Etcheber, H.: Exportation of organic carbon
654 from the Amazon River and its main tributaries, *Hydrological Processes*, 17(7), 1329–1344,
655 doi:10.1002/hyp.1287, 2003.
- 656 Nakićenović, N., Davidson, O., Davis, G., Grübler, A., Kram, T., Lebre La Rovere, E., Metz,
657 B., Morita, T., Pepper, W., Pitcher, H., Sankovski, A., Shukla, P., Swart, R. and Dadi, Z.:
658 IPCC Special report on emission scenarios, [online] Available from:
659 <http://www.ipcc.ch/ipccreports/sres/emission/index.php?idp=0>, 2000.
- 660 Nobre, A. D.: The Future Climate of Amazonia: Scientific Assessment Report, INPA and
661 ARA, São José dos Campos, Brazil. [online] Available from: [http://www.ccst.inpe.br/wp-](http://www.ccst.inpe.br/wp-content/uploads/2014/11/The_Future_Climate_of_Amazonia_Report.pdf)
662 [content/uploads/2014/11/ The_Future_Climate_of_Amazonia_Report.pdf](http://www.ccst.inpe.br/wp-content/uploads/2014/11/The_Future_Climate_of_Amazonia_Report.pdf) (Accessed 31
663 August 2015), 2014.
- 664 Potter, C., Klooster, S. and Genovese, V.: Carbon emissions from deforestation in the
665 Brazilian Amazon Region, *Biogeosciences*, 6(11), 2369–2381, 2009.
- 666 Randall, D. A., Wood, R. A., Bony, S., Colman, R., Fichet, T., Fyfe, J., Kattsov, V., Pitman,
667 A., Shukla, J., Srinivasan, J., Stouffer, R. J., Sumi, A. and Taylor, K. E.: Climate models and
668 their evaluation, in *Climate Change 2007: The Physical Science Basis. Contribution of*
669 *Working Group I to the Fourth Assessment Report of the Intergovernmental Panel on Climate*
670 *Change*, edited by S. Solomon, D. Qin, M. Manning, Z. Chen, M. Marquis, K. B. Averyt, M.
671 Tignor, and H. L. Miller, Cambridge University Press., 2007.
- 672 von Randow, C., Manzi, A. O., Kruijt, B., de Oliveira, P. J., Zanchi, F. B., Silva, R. L.,
673 Hodnett, M. G., Gash, J. H. C., Elbers, J. A., Waterloo, M. J., Cardoso, F. L. and Kabat, P.:
674 Comparative measurements and seasonal variations in energy and carbon exchange over
675 forest and pasture in South West Amazonia, *Theoretical and Applied Climatology*, 78(1-3),
676 5–26, doi:10.1007/s00704-004-0041-z, 2004.
- 677 Richey, J. E., Melack, J. M., Aufdenkampe, A. K., Ballester, V. M. and Hess, L. L.:
678 Outgassing from Amazonian rivers and wetlands as a large tropical source of atmospheric
679 CO₂, *Nature*, 416(6881), 617–620, doi:10.1038/416617a, 2002.

680 Rost, S., Gerten, D., Bondeau, A., Lucht, W., Rohwer, J. and Schaphoff, S.: Agricultural
681 green and blue water consumption and its influence on the global water system, *Water*
682 *Resources Research*, 44(9), doi:W09405 10.1029/2007wr006331, 2008.

683 Salimon, C. I., Davidson, E. A., Victoria, R. L. and Melo, A. W. F.: CO₂ flux from soil in
684 pastures and forests in southwestern Amazonia, *Global Change Biology*, 10(5), 833–843,
685 2004.

686 Sitch, S., Smith, B., Prentice, I. C., Arneth, A., Bondeau, A., Cramer, W., Kaplan, J. O.,
687 Levis, S., Lucht, W., Sykes, M. T., Thonicke, K. and Venevsky, S.: Evaluation of ecosystem
688 dynamics, plant geography and terrestrial carbon cycling in the LPJ dynamic global
689 vegetation model, *Global Change Biology*, 9(2), 161–185, doi:10.1046/j.1365-
690 2486.2003.00569.x, 2003.

691 Soares-Filho, B. S., Nepstad, D. C., Curran, L. M., Cerqueira, G. C., Garcia, R. A., Ramos, C.
692 A., Voll, E., McDonald, A., Lefebvre, P. and Schlesinger, P.: Modelling conservation in the
693 Amazon basin, *Nature*, 440(7083), 520–523, 2006.

694 Spracklen, D. V., Arnold, S. R. and Taylor, C. M.: Observations of increased tropical rainfall
695 preceded by air passage over forests, *Nature*, 489(7415), 282–285, doi:10.1038/nature11390,
696 2012.

697 Subramaniam, A., Yager, P. L., Carpenter, E. J., Mahaffey, C., Bjorkman, K., Cooley, S.,
698 Kustka, A. B., Montoya, J. P., Sanudo-Wilhelmy, S. A., Shipe, R. and Capone, D. G.:
699 Amazon River enhances diazotrophy and carbon sequestration in the tropical North Atlantic
700 Ocean, *Proceedings of the National Academy of Sciences*, 105(30), 10460–10465,
701 doi:10.1073/pnas.0710279105, 2008.

702 Thonicke, K., Spessa, A., Prentice, I. C., Harrison, S. P., Dong, L. and Carmona-Moreno, C.:
703 The influence of vegetation, fire spread and fire behaviour on biomass burning and trace gas
704 emissions: results from a process-based model, *Biogeosciences*, 7(6), 1991–2011,
705 doi:10.5194/bg-7-1991-2010, 2010.

706 Wagner, W., Scipal, K., Pathe, C., Gerten, D., Lucht, W. and Rudolf, B.: Evaluation of the
707 agreement between the first global remotely sensed soil moisture data with model and
708 precipitation data, *Journal of Geophysical Research*, 108(4611), doi:10.1029/2003JD003663,
709 2003.

710 Waterloo, M. J., Oliveira, S. M., Drucker, D. P., Nobre, A. D., Cuartas, L. A., Hodnett, M. G.,
711 Langedijk, I., Jans, W. W. P., Tomasella, J., de Araújo, A. C., Pimentel, T. P. and Estrada, J.
712 C. M.: Export of organic carbon in run-off from an Amazonian rainforest blackwater
713 catchment, *Hydrological Processes*, 20(12), 2581–2597, 2006.

714 Worbes, M.: The forest ecosystem of the floodplains, in *The Central Amazon Floodplain*,
715 edited by W. J. Junk, pp. 223–265, Springer, Berlin, Germany., 1997.

716

717

718

719 **6 Tables**

720 **Table 1: Location and characteristics of the three sub-regions.**

	<i>North-West corner</i>	<i>South-East corner</i>	<i>area [10³km²]</i>	<i>changes in inundation length*</i>	<i>changes inundated area*</i>	<i>land use intensity</i>
R1	0.5°S / 78.5°W	7.0°S / 72°W	523.03	1 month longer	larger	low
R2	1.0°S / 70.0°W	5.0°S / 52°W	891.32	±½ month shift	heterogeneous	medium
R3	4.5°S / 58.0°W	11.0°S / 52°W	523.03	½ month shorter	smaller	high

721 Regions are depicted in Figure 2. * Changes in inundation compared to the average of 1961-
722 1990, as estimated and discussed in Langerwisch et al. (2013)

723

724

725 **Table 2: Basin-wide (B) and region wise (R1-R3) amount of carbon in POC and DOC,**
 726 **outgassed carbon and IC [10^{12} g month⁻¹] averaged over 30 years and five climate**
 727 **models.**

	NatVeg _{ref}	NatVeg _{fut}	GOV _{futA/B}	BAU _{futA/B}	GOV _{futA2}	BAU _{futA2}	GOV _{futB1}	BAU _{futB1}
POC								
B	1.64±0.06	1.76±0.51	1.52±0.43	1.28±0.35	1.63±0.41	1.39±0.34	1.55±0.31	1.30±0.24
R1	0.16±0.01	0.22±0.05	0.20±0.05	0.20±0.05	0.21±0.05	0.21±0.05	0.18±0.02	0.18±0.02
R2	0.42±0.01	0.43± 0.15	0.37±0.12	0.30±0.09	0.40±0.13	0.33±0.10	0.38±0.09	0.31±0.07
R3	0.15±0.01	0.14±0.05	0.11±0.04	0.07±0.03	0.12±0.04	0.08±0.02	0.12±0.03	0.08±0.02
DOC								
B	3.41±0.13	3.58±1.05	3.07±0.87	2.59±0.71	3.29±0.84	2.77±0.69	3.15±0.63	2.64±0.48
R1	0.34±0.02	0.46±0.11	0.43±0.10	0.42±0.10	0.45±0.10	0.44±0.10	0.39±0.05	0.38±0.05
R2	0.93±0.03	0.91±0.32	0.77±0.26	0.64±0.20	0.84±0.27	0.69±0.21	0.81±0.20	0.66±0.15
R3	0.34±0.02	0.30±0.11	0.24±0.09	0.16±0.06	0.26±0.08	0.17±0.05	0.27±0.07	0.17±0.04
outgassed carbon								
B	11.82±0.41	16.63±4.14	14.30±3.44	12.05±2.76	15.75±3.43	13.24±2.80	13.37±2.20	11.15±1.68
R1	1.15±0.06	2.05±0.38	1.93±0.35	1.91±0.35	2.10±0.35	2.08±0.35	1.61±0.13	1.60±0.14
R2	2.52±0.08	3.36±0.99	2.81±0.78	2.37±0.6	3.09±0.85	2.59±0.66	2.66±0.56	2.22±0.43
R3	0.99±0.04	1.12±0.42	0.91±0.34	0.55±0.20	1.03±0.32	0.62±0.18	0.94±0.26	0.56±0.14
IC								
B	0.227±0.003	0.457±0.119	0.457±0.120	0.456±0.121	0.523±0.137	0.522±0.138	0.365±0.063	0.364±0.064
R1	0.005±0.001	0.016±0.003	0.013±0.003	0.013±0.003	0.015±0.004	0.015±0.004	0.009±0.001	0.009±0.001
R2	0.153±0.002	0.308±0.081	0.308±0.082	0.307±0.083	0.351±0.094	0.350±0.096	0.245±0.044	0.244±0.044
R3	0.006±0.000	0.011±0.003	0.011±0.003	0.011±0.003	0.013±0.003	0.013±0.003	0.009±0.001	0.009±0.001

728 'ref' refers to mean amounts during reference period 1971-2000. 'fut' refers to mean amounts
 729 during future period 2070-2099. Values given are the mean ± standard deviation of the five
 730 climate models.

731

732

733

Table 3: Proportion [%] of area dominated by climate or land use change impacts.

	<i>significantly changed fraction</i>			<i>climate change dominated¹</i>			<i>land use change dominated¹</i>			<i>balanced¹</i>		
	<i>A1B</i>	<i>A2</i>	<i>B1</i>	<i>A1B</i>	<i>A2</i>	<i>B1</i>	<i>A1B</i>	<i>A2</i>	<i>B1</i>	<i>A1B</i>	<i>A2</i>	<i>B1</i>
POC												
GOV	50.85	50.91	50.86	58.8	58.7	54.9	40.9	40.7	44.6	0.3	0.6	0.5
BAU	50.80	50.85	50.85	42.3	43.7	40.1	57.5	56.2	59.8	0.2	0.1	0.1
IC												
GOV	50.80	50.80	50.80	100.0	100.0	100.0	0.0	0.0	0.0	0.0	0.0	0.0
BAU	50.80	50.80	50.80	100.0	100.0	100.0	0.0	0.0	0.0	0.0	0.0	0.0
outgassed carbon												
GOV	97.6	97.60	97.61	70.5	77.7	68.4	29.3	22.3	31.1	0.2	0.0	0.4
BAU	97.55	97.65	97.60	52.4	56.9	50.2	47.6	43.0	49.7	0.1	0.1	0.1

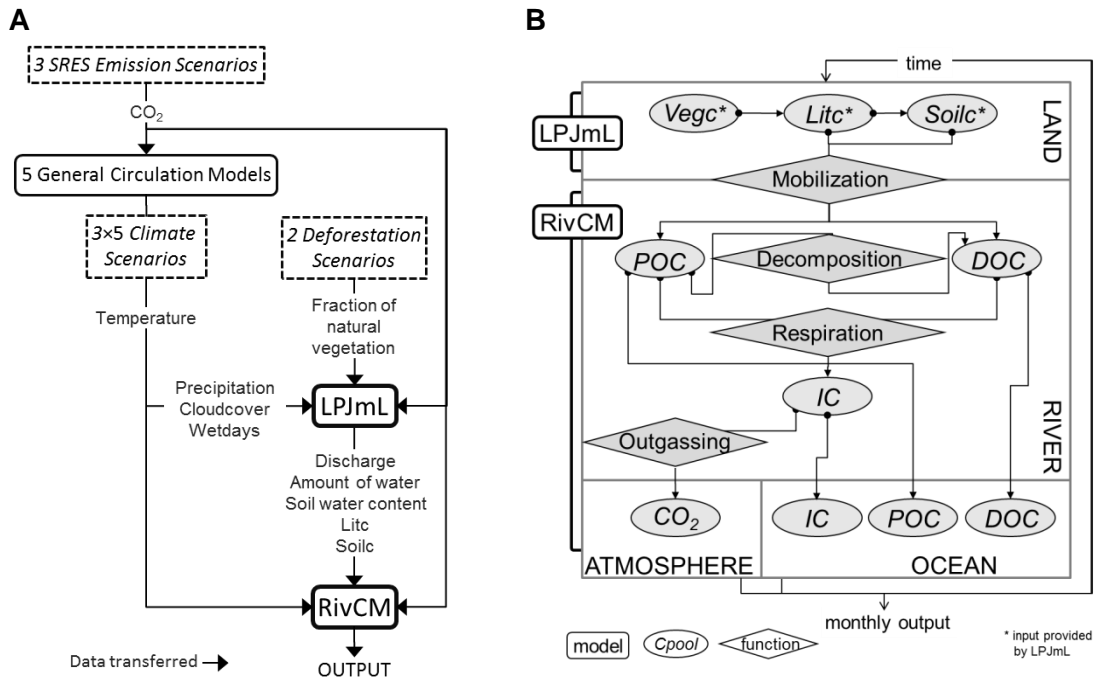
734

If both impacts compensate each other the cell is balanced. ¹The proportions refer to the

735

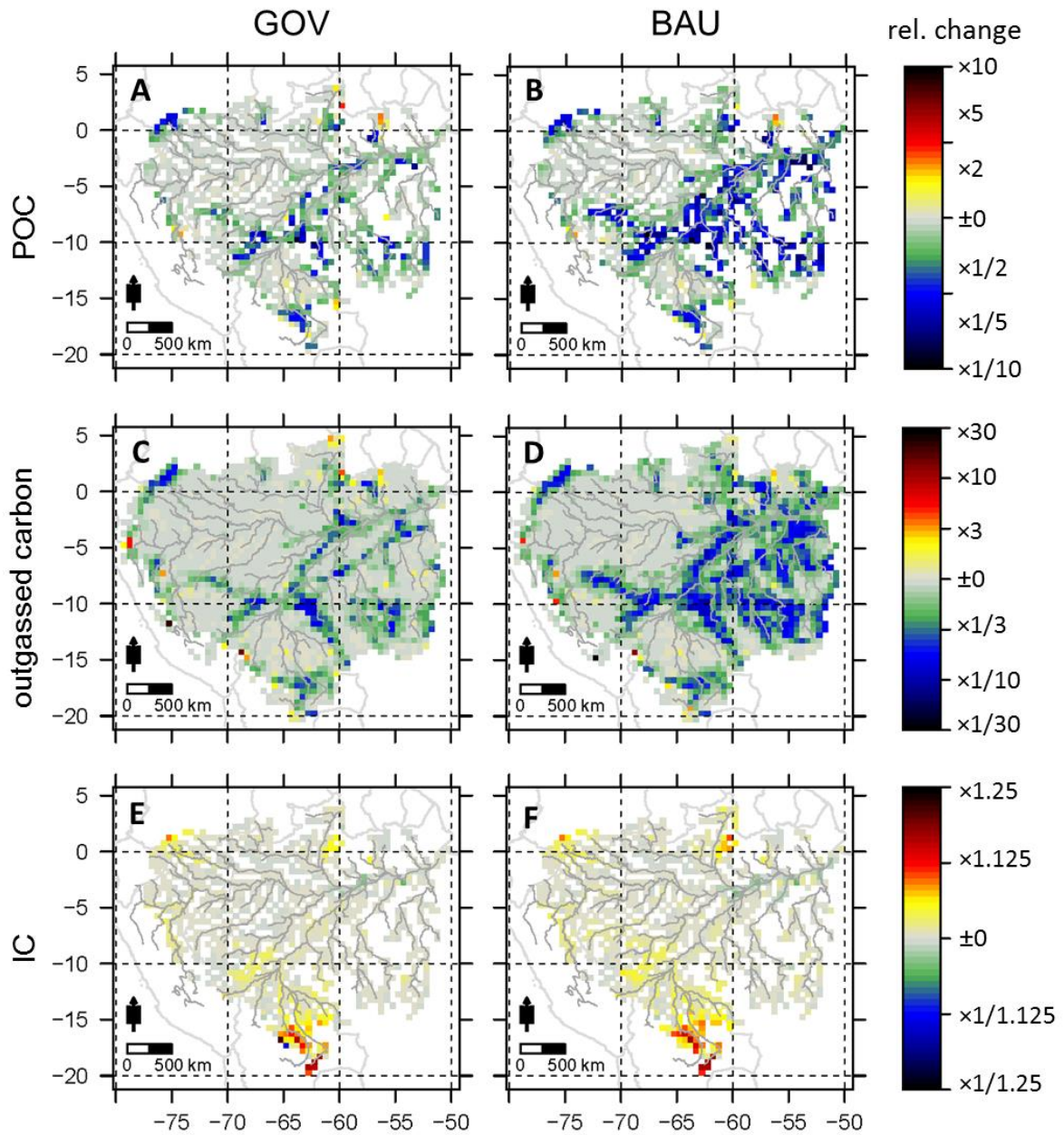
significantly changed overall fraction (first columns).

736 **7 Figures**



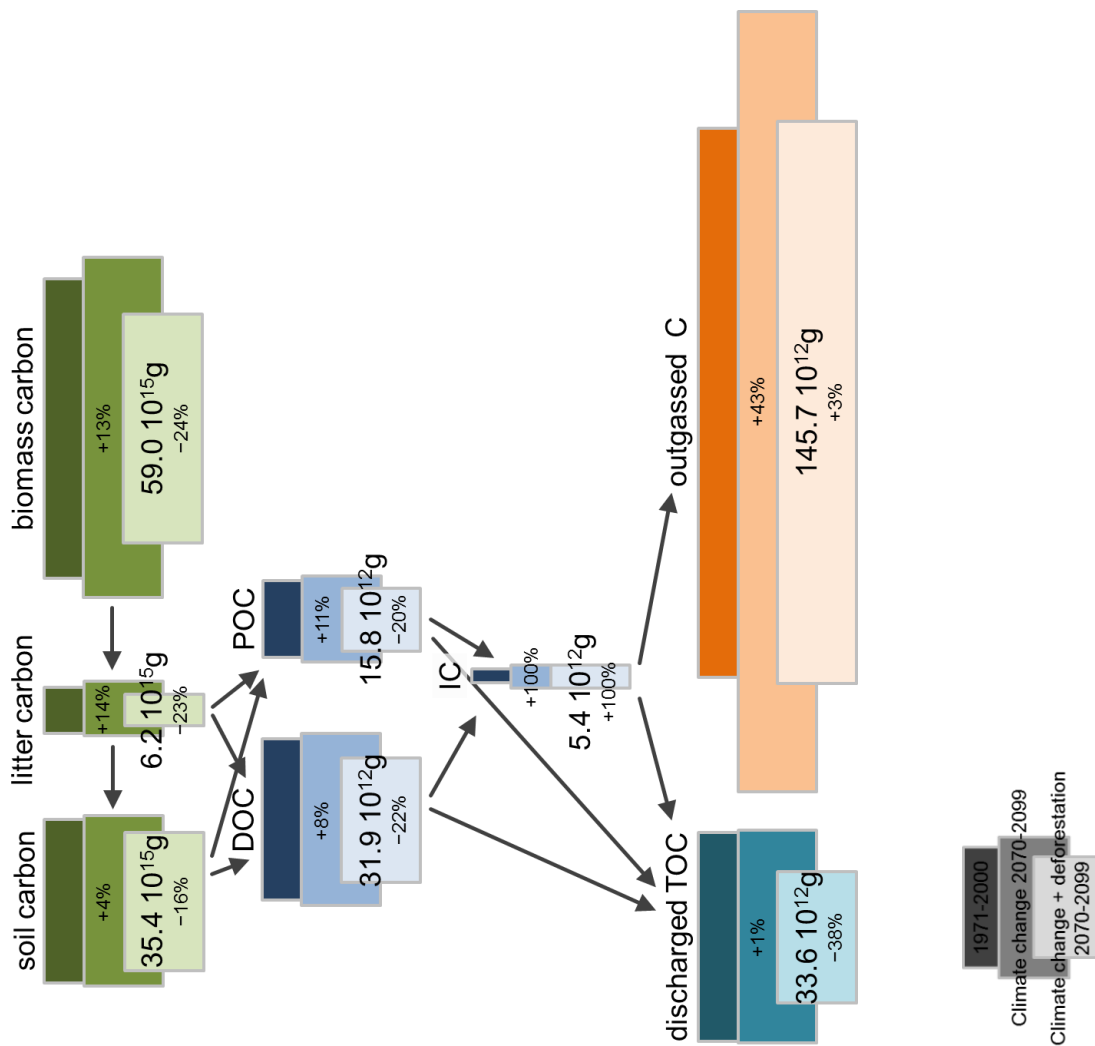
737 **Figure 1: Overview of the general transfer of data between scenarios and models (A)**
 738 **and the detailed calculation of carbon fluxes within and between LPJmL and RivCM.**

739
 740



741

742 **Figure 2: Change in carbon caused by deforestation.** Climate model mean (E_{Defor}) of the
 743 change of particulate organic carbon POC (A, B), outgassed carbon (C, D) and inorganic
 744 carbon IC (E, F). Results of the SRES emission scenario A1B are averaged over five climate
 745 models. Areas in yellow and red indicate a gain and areas in green and blue indicate a loss in
 746 carbon caused by deforestation (GOV and BAU).

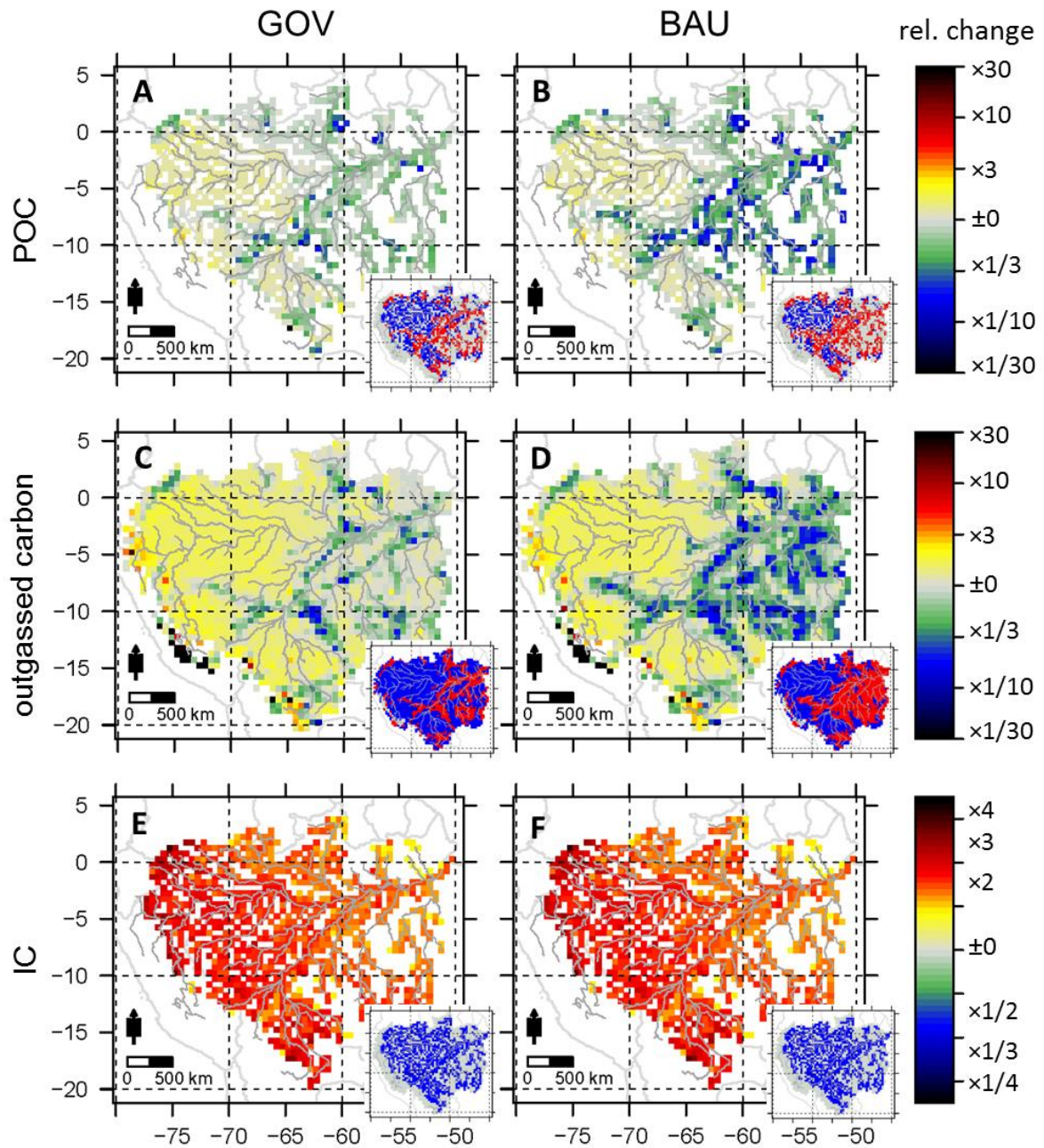


748

749 **Figure 3:** Averaged annual amounts and change in the basin carbon budget due to
 750 **climate change and deforestation.** Dark boxes indicate the amount of carbon during the
 751 reference period (1971-2000), intermediate boxes during the future period (2070-2099) under
 752 climate change only (Langerwisch et al., 2015), light boxes during the future period under the
 753 forcing of climate change and deforestation together (average over all SRES scenarios and
 754 GCMs). Amount is given for future period with relative change compared to reference.
 755 Arrows indicate the direction of carbon transfer.

756

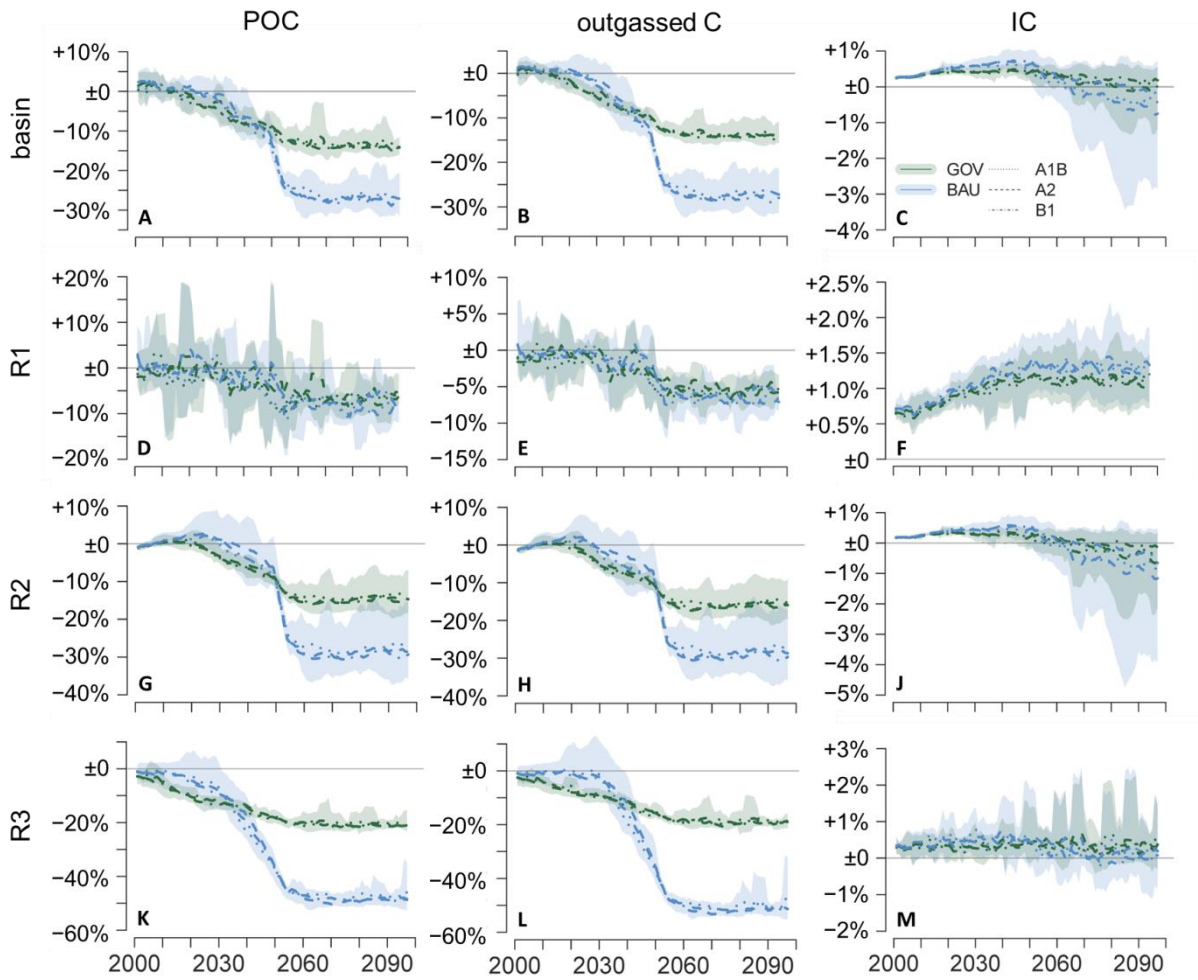
757



758

759 **Figure 4:** Change in carbon caused by deforestation and climate change. Climate model
 760 mean ($E_{CCDefor}$) of the change of particulate organic carbon POC (A, B), outgassed carbon (C,
 761 D) and inorganic carbon IC (E, F). The inset maps show blue areas where changes are
 762 predominantly caused by climate change and red areas where changes are predominantly
 763 caused by deforestation. For further details see Figure 2.

764



766

767

768

769

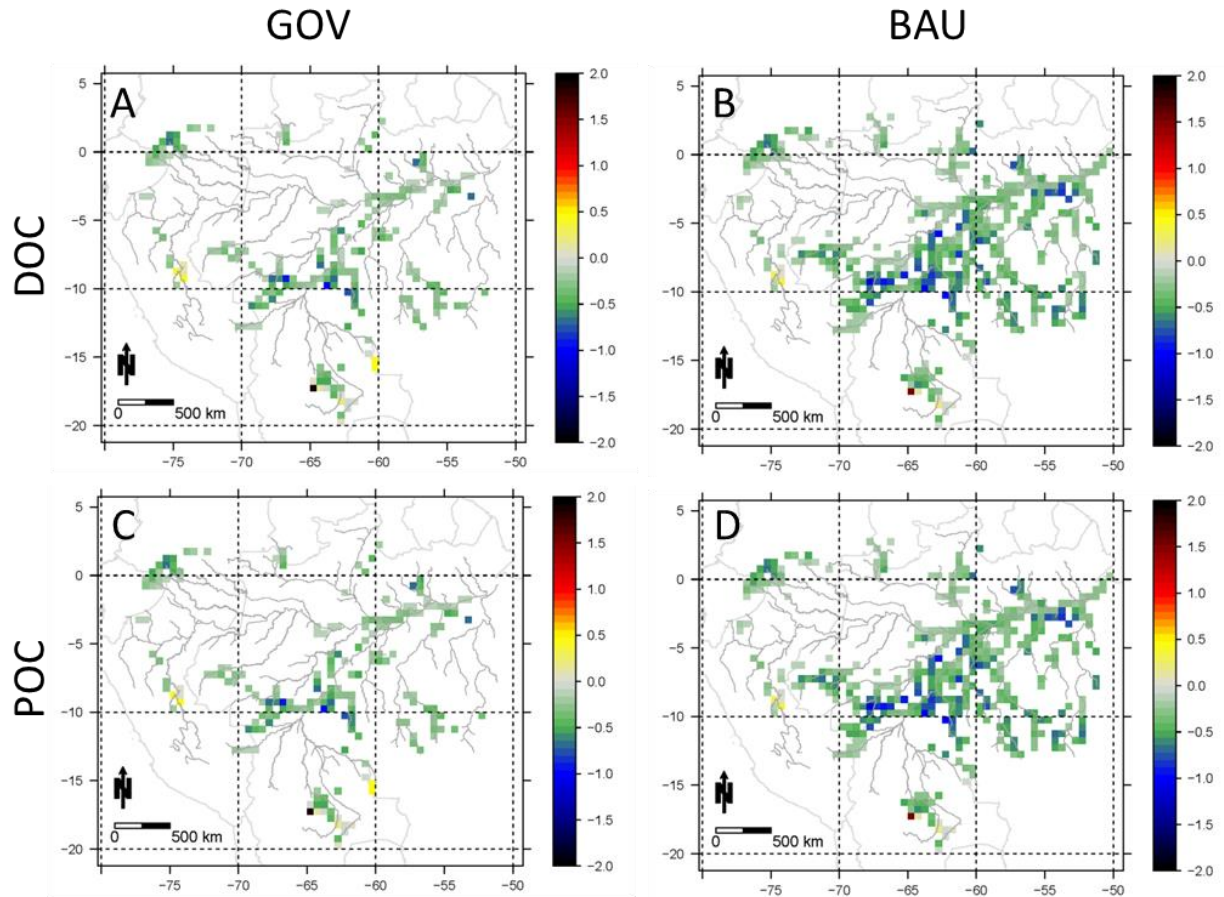
770

771

772

773

Figure 5: Temporal change in particulate organic carbon due to land use change. Change of annual sum of carbon in the deforestation scenario (GOV or BAU) compared to the NatVeg scenario (average over 1971-2000) for the whole basin (A-C) and the three sub-regions (R1-R3; D-M) as 5-year-mean for GOV (green) and BAU (blue). The shaded areas indicate the full range of values of all five climate models. Bold lines represent the 5-year-mean of the five climate models.



774

775 **Figure S1: Similar change in dissolved (A, B) and particulate organic carbon (C, D) due**
 776 **to deforestation.** SRES scenario is A1B, climate model is MPI-ECHAM5. Positive values
 777 (yellow and red) indicate a gain and negative values (green and blue) indicate a loss in carbon
 778 caused by deforestation (GOV and BAU). Only cells with significant changes ($p < 0.05$,
 779 Wilcoxon Rank Sum Test) are shown.

780